Supporting Information

Comparative Assessment of FTO and ITO Substrates for $BiVO_4$ Photoanodes: Superior Surface Quality Enabling Faster Water Oxidation in ITO

Yeon Gyo Shim[1,2], Yuki Nakatsukasa[3], Kana Matsumoto[3], Ji Eun Kim[1], Su Jin Kim[1], Seung Heon Choi[1,2], Seung Hyeon Jeong[1,2], Seong Kyu Jang[1,2], Aram Hong[2], Kenji Katayama[3], Woon Yong Sohn[1,2]*

1. Department of Chemistry, Chungbuk National University, Chungdae-ro 1, Cheongju, Chungbuk 28644, Korea
2. Chungbuk National University G-LAMP Project Group, Chungdae-ro 1, Cheongju, Chungbuk 28644, Korea
3. Department of Applied Chemistry, Faculty of Science and Technology, Chuo University, 1-13-27 Kasuga, Bunkyo, Tokyo 112-8551, Japan

*Corresponding author:

W. Y. Sohn, Phone: 82-43-261-2285, E-mail: nunyong@chungbuk.ac.kr

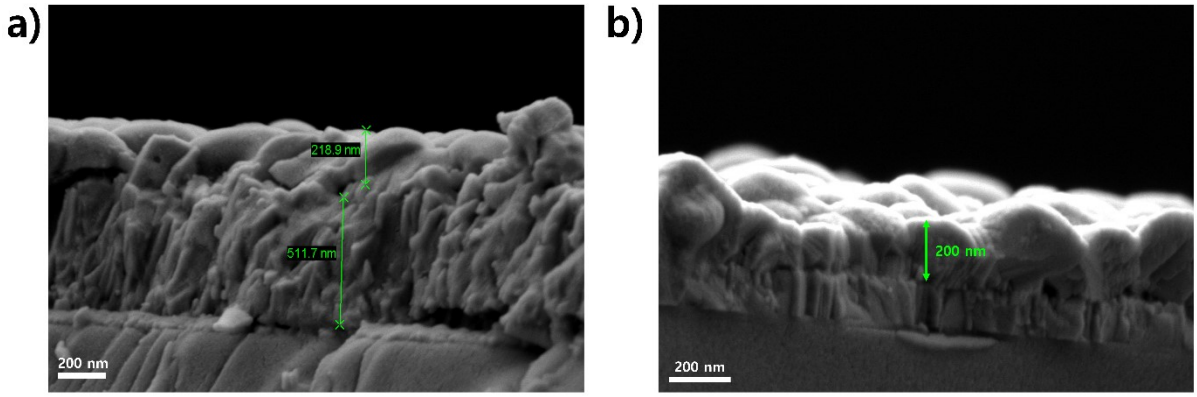

Fig. S1. Cross-sectional SEM images of a) the F/B and b) the I/B films.

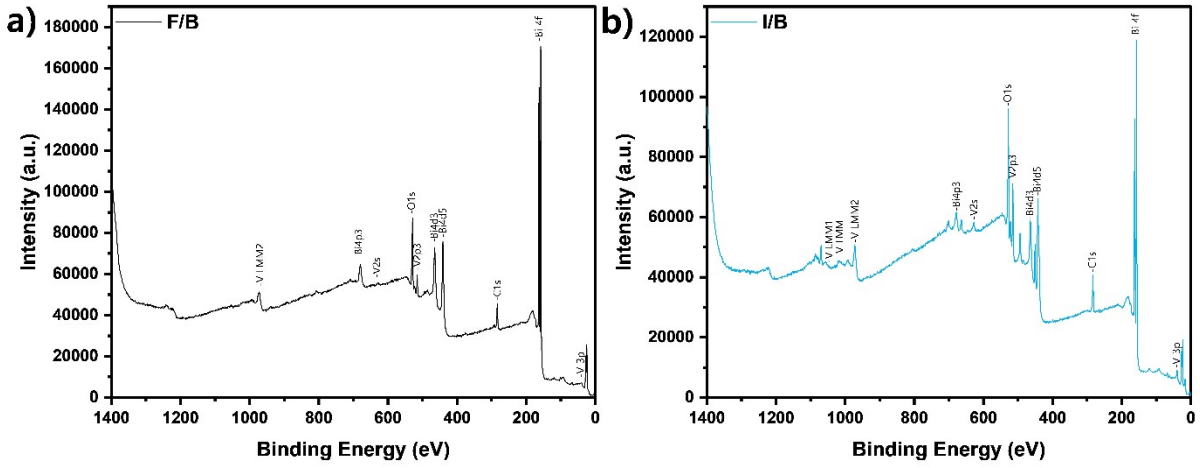

Fig. S2. XPS survey spectra of a) the F/B and b) the I/B.

Table S1. The binding energies of V 2p and Bi 4f for the F/B and the I/B.

	F/B Binding energy (eV)	I/B Binding energy (eV)
V $2p_{3/2}$	516.88	516.89
V $2p_{1/2}$	524.35	524.19
Bi $4f_{7/2}$	159.28	159.28
Bi $4f_{5/2}$	164.58	164.59

Table S2. The binding energies, peak intensities, and FWHM of O 1s (O_L, O_V, O_A) for the F/B and the I/B.

		F/B	I/B
O_L	Binding energy (eV)	530.1	529.9
	Intensity (a.u.)	10238.3	10699.3
	FWHM	1.1252	1.5373
O_V	Binding energy (eV)	531.4	531.4
	Intensity (a.u.)	3304.6	1682.2
	FWHM	1.6406	1.6403
O_A	Binding energy (eV)	532.5	532.5
	Intensity (a.u.)	1032.4	461.5
	FWHM	1.2491	1.2491

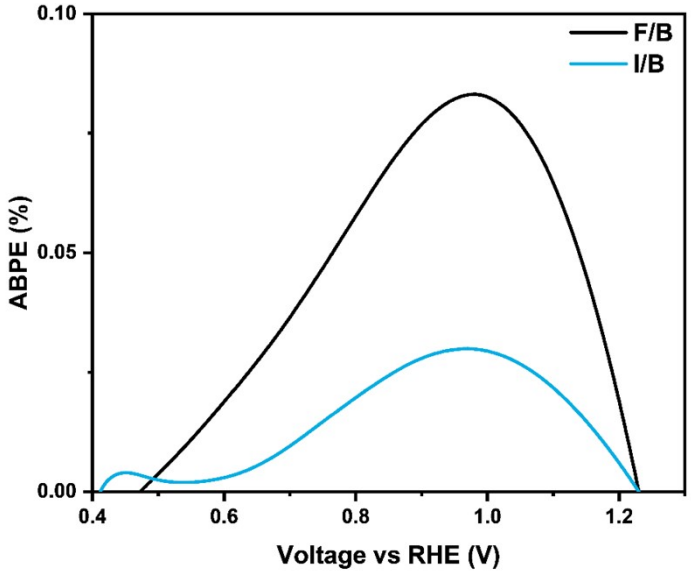

Fig. S3. The applied bias photon-to-current efficiencies (ABPEs) of the F/B (black) and the I/B (blue).

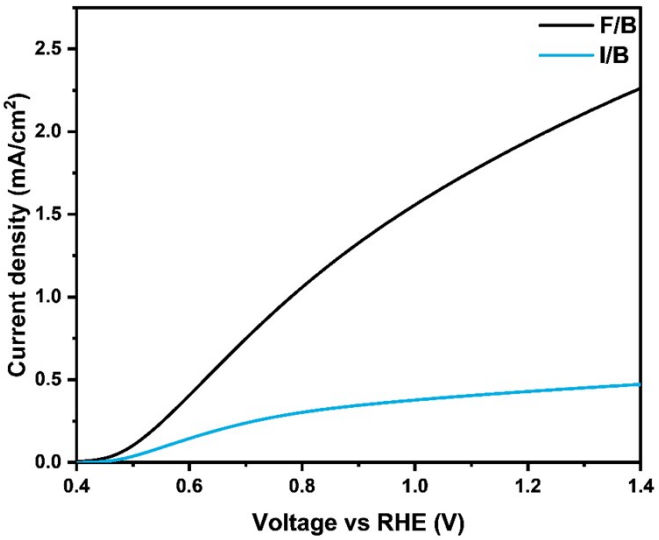

Fig. S4. The J-V curves of the F/B(black) and the I/B (blue) measured in presence of Na_2SO_3 (0.2 M).

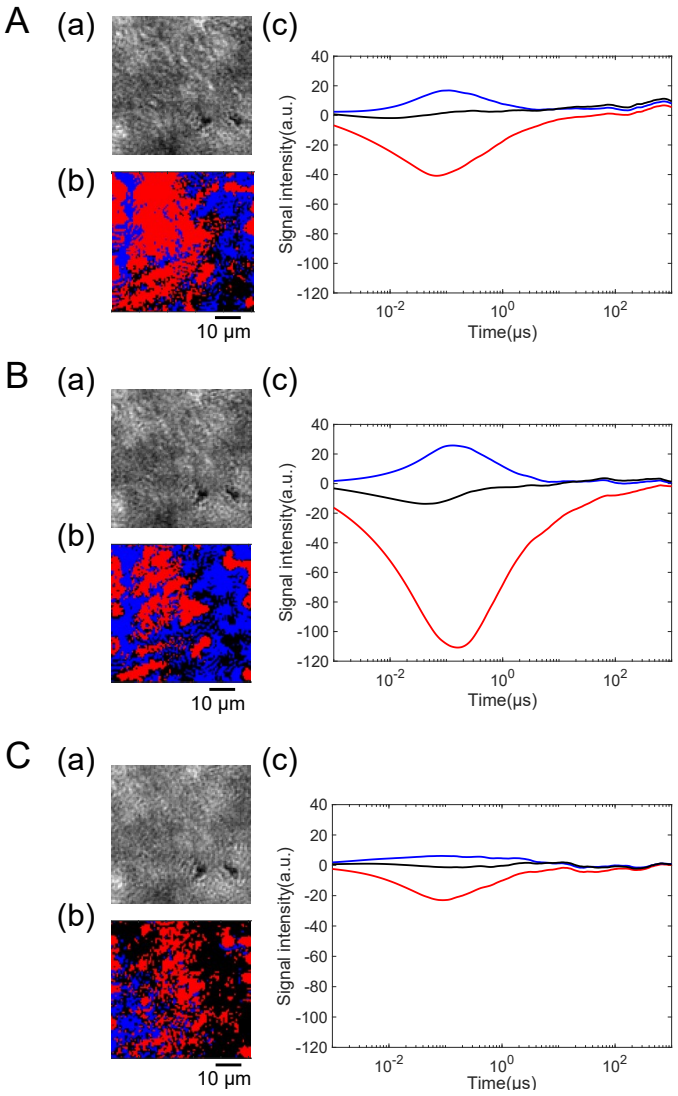

D

Solvent	Category	Ratio [%]	Rise [ns]	Decay [μs]
ACN	1 (Red)	46	9 ± 1	0.6 ± 0.1
	2 (Blue)	29	25 ± 2	0.7 ± 0.1
	3 (Black)	25	-	-
EtOH	1 (Red)	27	16 ± 1	1.2 ± 0.1
	2 (Blue)	44	27 ± 2	0.8 ± 0.1
	3 (Black)	29	-	-
NB/ EtOH	1 (Red)	28	8 ± 1	0.7 ± 0.1
	2 (Blue)	13	6 ± 1	2.5 ± 0.1
	3 (Black)	59	-	-

Fig. S5. The clustering analyses of the charge carrier responses of the F/B in (A) ACN, (B) EtOH, and (C) NB/EtOH and the corresponding categorized map is shown in (b), and the scale bar corresponds to 10 μm. The averaged responses for the categorized responses are shown in (c). The area ratios of categories and the rise/decay times for the categories are shown in (D).

We found two categories of responses; a rise-and-decay response with rise and decay time constants of 9±1 ns and 0.6±0.1 μs (red), and a valley-and-recovery response with a fall and recovery time constants of 25±2 ns and 0.7±0.1 μs (blue) along with no-response regions (black). The signal with an opposite sign of the refractive index change indicates that the responses had a different origin of charge carriers, and each response was attributed to either electrons or holes. By introducing the hole scavenger, EtOH, the red region decreased, indicating this corresponded to the hole dynamics. On the other hand, the region of the blue decreased by introducing an electron scavenger (NB), and thus the positive response (blue) corresponded to the electron response.

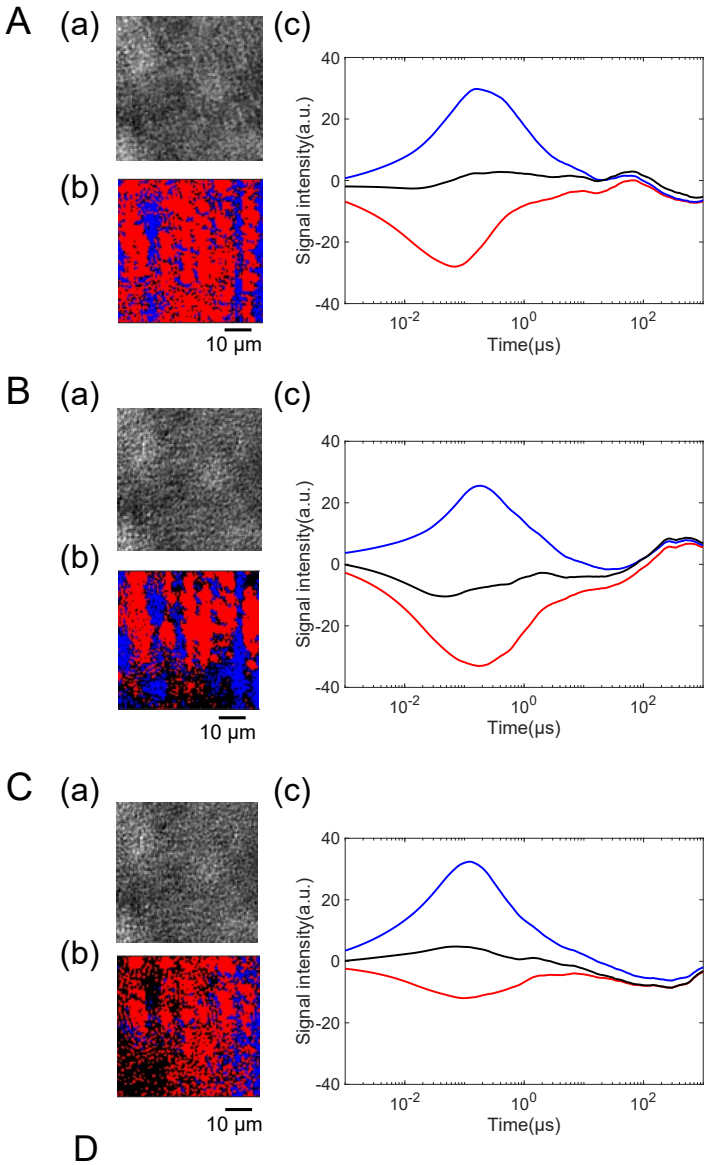

D

Solvent	Category	Ratio [%]	Rise [ns]	Decay [μs]
ACN	1 (Red)	64	9 ± 1	0.3 ± 0.1
	2 (Blue)	24	31 ± 2	1.3 ± 0.1
	3 (Black)	12	-	-
EtOH	1 (Red)	40	15 ± 1	1.5 ± 0.1
	2 (Blue)	26	42 ± 3	0.9 ± 0.1
	3 (Black)	34	-	-
NB/ EtOH	1 (Red)	46	13 ± 1	0.9 ± 0.1
	2 (Blue)	12	18 ± 2	0.6 ± 0.1
	3 (Black)	42	-	-

Fig. S6. The clustering analyses of the charge carrier responses of the I/B in (A) ACN, (B) EtOH, and (C) NB/EtOH and the corresponding categorized map is shown in (b), and the scale bar corresponds to 10 μm. The averaged responses for the categorized responses are shown in (c). The area ratios of categories and the rise/decay times for the categories are shown in (D).

In ACN, we found three categories of responses a single rise-and-decay response with rise and decay time constants of 9±1 ns and 0.3±0.1 μs (red), a valley-and-recovery response with fall and recovery time constants of 31±2 ns and 1.3±0.1 μs (blue), and no-response regions (black). By introducing a hole scavenger, EtOH, the red response decreased, indicating the red response corresponded to the surface trapped holes scavenged by EtOH. The blue response disappeared in NB/EtOH, indicating that this component corresponded to the electron dynamics.

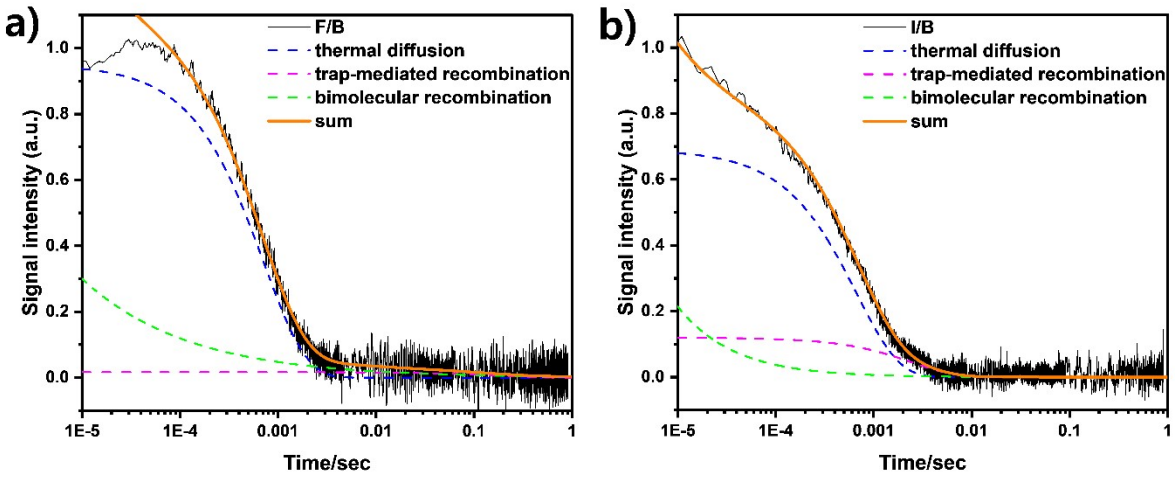

Fig. S7. The NF-HD-TG responses of a) the F/B and b) the I/B with the grating spacings (Λ) of 70 μm.

Table S3 List of time constants of each component of the F/B and the I/B at the grating spacing of 70 μm.

	$\tau_1\ (\times 10^{-4}\ s)$	$\tau_2\ (\times 10^{-2}\ s)$
F/B	7.14	16.2
I/B	6.7	0.25